Journal of Nanobiotechnology

RESEARCH

Open Access

IFITM1 is a host restriction factor that inhibits porcine epidemic diarrhea virus infection

Jiahao Cheng[1†], Jiayi He[1†], Simeng Feng[1], Lei Tan[1,3], Binghan Bai[1], Wei Dong[1], Bin Li[4], lixin Wen[1,5,6], Aibing Wang[1,2] and Xiaomin Yuan[1*]

Abstract

Background Porcine epidemic diarrhea virus (PEDV) infection and transmission pose a serious threat to the global swine industry. The search for a new host factor with anti-PEDV effect may be an effective potential target for the development of novel antiviral drugs. Interferon-induced transmembrane proteins (IFITMs) play a crucial role in the innate immune response triggered by viral infection, and it has been suggested that IFITMs can block the early stages of viral replication, but the mechanism of action is currently unclear. The current study sheds light on the role of IFITM1 in PEDV infection. Specifically, overexpression of IFITM1 suppresses PEDV proliferation in IPEC-J2 cells, while knockdown of IFITM1 has the opposite effect. Collectively, these findings underscore IFITM1's inhibitory role in PEDV infection, with critical implications for the residues and structural motifs within its CTD.

Results The study demonstrates that IFITM1, an interferon-induced transmembrane protein, plays a critical role in the antiviral response against Porcine Epidemic Diarrhea Virus (PEDV). Notably: Overexpression of IFITM1 suppresses PEDV proliferation.IFITM1 co-localizes with PEDV virions in the cytoplasm surrounding the nucleus.Immunocolloidal gold electron microscopy reveals IFITM proteins embedded on the surface of PEDV virions.IFITM1 directly interacts with the N protein of PEDV.C-terminal domain mutations in IFITM1 compromise its inhibitory function against PEDV, with specific amino acid residues playing a pronounced role.These findings enhance our understanding of innate immunity and antiviral defense mechanisms, with potential implications for therapeutic strategies against PEDV infection.

Conclusions The study establishes IFITM1 as a key player in the antiviral response against PEDV. Its inhibitory function, co-localization with virions, and interaction with the N protein provide valuable insights. Notably, the CTD mutations of IFITM1 have a fundamental impact on its modulatory action. These findings contribute to our understanding of innate immunity and antiviral defense mechanisms, with potential implications for therapeutic strategies against PEDV infection.

Keywords Innate immunity, Interferon-induced transmembrane protein 1, Porcine epidemic diarrhea virus, Antiviral infection, Immune-gold labeling

[†]Jiahao Cheng and Jiayi He have contributed equally to this work and share first authorship.

*Correspondence:
Xiaomin Yuan
yxm1230@hunau.edu.cn
Full list of author information is available at the end of the article

Graphical Abstract

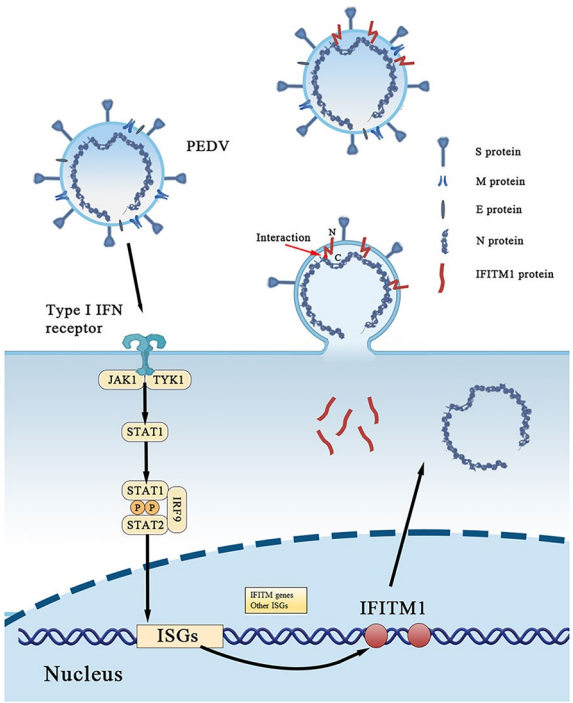

Introduction

PEDV, a leading causative agent of porcine epidemic diarrhea, is an enveloped, single stranded, positive-sense RNA virus that belongs to the order of Nidovirales, family of Coronaviridae and genus of Alphacoronavirus [17]. This virus primarily infects small intestinal epithelial cells in vivo and causes acute diarrhea, vomiting, dehydration and high mortality in neonatal piglets [15]. Vaccination is regarded the best and effective method to prevent and control PEDV, while the inactivated or live attenuated vaccines based on PEDV CV777 strain [23] failed to provide effective protection against gastroenteric pathogens [15]. This issue deriving from antigenic variations between the traditional attenuated vaccines and the current highly virulent PEDV field strains [18], together with the fact of special features of the porcine intestinal mucosal immune system, highlight to urgently develop updated PEDV vaccines and in-depth study the host innate immunity which is susceptible to the influence of the viral components.

In this regard, interferon induced transmembrane proteins (IFITM), a class of interferon stimulated genes (ISGs) expressed proteins, have been considered as one of the critical antiviral proteins in innate immunity [15], and their expression is significantly upregulated by the induction of type I and II interferons. Though the amino acid sequences of IFITMs family members are highly conserved, they can still be divided into 3 categories in accordance with the similarity of amino acid sequences and the differences of protein functions. The first and important category is mainly related to innate immunity, including IFITM1, IFITM2 and IFITM3 [8, 22]. These proteins are widely distributed in cells, while the location and content of them present a wide variation, probably due to the difference in the N-terminal domain (NTD) sequences, e.g. the NTD of IFITM2 and IFITM3 are 20 and 21 amino acids longer than IFITM1, respectively [8]. Previous study has indicated that IFITM1 is located predominantly in the lipid rafts of the plasma membrane and early endosome membrane, whereas IFITM2 and IFITM3 are mostly located in the late endosome membrane [16]. Previous studies have confirmed that IFITMs have the capability to suppress the entry of viruses through inhibiting the hemifusion of viral membrane and host cell membranes [9] or restricting the formation of fusion pores following virus-endosome hemi fusion [1, 19]. Notably, the differences in the subcellular localization and organelle distribution of IFITMs allow them to display selectivity in the inhibition of distinct viruses, and various sensitivity even to the same virus. For example,

when the target of membrane fusion is located on the plasma membrane, the inhibitory efficiency of IFITM1 on HIV invasion into the cells was better than these of IFITM2 and IFITM3 [5]. Likewise, IFITM3 had stronger suppressive effect on influenza virus infection, as compared with IFITM1 and IFITM2 [7]. These suggest that IFITMs have distinct antiviral functions, relying on the individual member and the infected virus(s).

Moreover, the correct subcellular localization of IFITMs is closely related to their antiviral activity [13, 21]. For instance, mutation of IFITM3 tyrosine 20 resulted in incorrect subcellular localization of this protein, thereby abrogating its antiviral activity to influenza A virus and DENV [14], and enhancing the entry of SARS-CoV [28]. IFITM1 is located on the surface of the cell membrane and can effectively inhibit the early invasion of the disease to reach a peak in 24 h. In the early endosomes and lysosomes of IFITM3, the early inhibition effect on PEDV was not as significant as that of IFITM1. Likewise, the palmitoylation at 72 cysteine of IFITM3 is important for its subcellular localization and antiviral activity [10]. In addition to mutations or modifications, some specific motifs such as the 122KRXX125 motif at the C-terminal domain (CTD) have fundamental effect on the antiviral function of IFITMs [24]. The KRRK motif of IFITM1 affects the function in inhibiting Zika virus infection, while the 127–132 amino acid residues in the CTD domain of IFITM3 regulate its ability to inhibit HIV-1 invasion of cells [2]. These demonstrate that any alteration including mutations, modifications and motifs severely influence the antiviral action of IFITMs.

Though antiviral mechanisms of IFITMs remains to be further investigated, a confirmed one is that they are able to protect target cells from the entry or invasion of viruses, as aforementioned. A proposed one is that then can affect the later stages of the viral replication cycle. During the infection of HIV-1, the presence of IFITMs in virus producing cells allows them to be incorporated into HIV-1 virion particles, thus decreasing the particle infectivity. Consequently, the main functions of IFITMs are currently considered to suppress virus entry and reduce the infectivity of nascent viruses [6].

So far, the antiviral activities of IFITMs have been validated in the infections of numerous viruses, such as respiratory syncytial virus (RSV) [21], ebolavirus (EBOV) and severe acute respiratory syndrome virus (SARS-CoV) [12, 20], pseudorabies virus [26]. Notably, most studies associated with antiviral actions of IFITMs focused on the IFITM3 protein, with human viruses as an emphasis, however, the investigations on other IFITM members like IFITM1 remained relatively few. Given the critical role of IFITM1 in innate immunity and the severity of Porcine epidemic diarrhea virus (PEDV) in the healthy development of pig industry worldwide, this study intended to address the potential function of IFITM1 in PEDV infection. Our results elucidated the antiviral mechanism of IFITM1 during PEDV infection and the key functional residues at the CTD of the molecule, thereby suggesting that IFITM1 may be a potential novel antiviral therapeutic target.

Materials and methods

Antibodies, chemicals, and reagents

Antibodies against β-actin, HA-tag and FLAG-tag were purchased from Cell Signaling Technology, anti-PEDV was provided by Qianxun Biology, and anti-IFITM was prepared in the laboratory. FITC (fluorescein isothiocyanate)-conjugated goat anti-mouse IgG and goat anti-rabbit IgG were purchased from Li-COR Biosciences.

Cells and viruses

IPEC-J2 or 293 T cells were cultured at 37 ℃ with 5% CO_2 in 1640 or DMEM, respectively, supplemented with 10% fetal bovine serum (FBS) and 1% penicillin–streptomycin. The PEDV strain JS2008 was provided by the Veterinary Research Institute of Jiangsu Academy of Agricultural Sciences (Nanjing, China).

Establishment of pIFITM1 stable cell line

The fragment coding pIFITM1 or pIFITM2 or pIFITM3 was individually amplified by PCR using cDNAs prepared from PK15 cells as the template and the primers listed in Table 1. The PCR products were separately cloned into the XbaI and BamHI sites of the pLVML-Myc-MCS-IRES-Puro lentiviral vector to generate pLVML-Myc-IFITM1/2/3-IRES-Puro. On day 0, human HEK293T cells were seeded into 10 cm dishes at a density of 4×10^6 per dish. On day 1, cells were transfected with 10 μg/dish recombinant plasmid, 5 μg/dish psPAX2 (packaging plasmid), and 5 μg/dish pMD2.G (envelope plasmid) using

Table 1 Primers for amplifying wild-type of swine IFITM1, 2, 3

Name	Sequence (5′-3′)
pIFITM1-F	TGCTCTAGAATGATCAAGAGCCAGCACGAGATGGAC
pIFITM1-R	CGGGATCCTTAGTGGTGGTGGTGGTGGTGCTAGTAGC CTCTGTTACTCTTTGCGCG
pIFITM2-F	TGCTCTAGAATGAACTGCGCTTCCCAGCCCTTCTTC
pIFITM2-R	CGGGATCCTTAGTGGTGGTGGTGGTGGTGCTAGTAG CCTCTGTTACTCTTTGCGCG
pIFITM3-F	TGCTCTAGAATGAATTGCGCTTCCCAGCC
pIFITM3-R	CGGGATCCTTAGTGGTGGTGGTGGTGGTGCTAGTAG CCTCTGTAATCCT

Lipofectamine 2000 (Invitrogen, Grand Island, NY, USA). On day 3, the culture media containing lentiviruses were collected and used to infect IPEC-J2 cells. Then, the lentivirus infected cells were subjected to the treatment of puromycin (3 μg/ml) for 7 days. Finally, the expression of IFITM proteins was detected by Western blotting using HRP-conjugated anti-Myc antibody.

RNA interference (RNAi)

On day 0, human HEK293T cells were seeded in 10 cm dishes at 4×10^6 per dish. On day 1, the cells were transfected with 10 μg/dish short hairpin RNA (shRNA) plasmid (Table 2), 5 μg/dish psPAX2 (packaging plasmid), and 5 μg/dish pMD2.G (envelope plasmid) using Lipofectamine 2000. On day 3, the culture media containing viruses were collected, filtered through a 0.45 μm membrane, and stored at 80 ℃. For cell infection, IPEC-J2 cells were cultured in T25 flasks. When the cells reached a confluence of 70–80%, they were infected with 1 ml lentivirus-containing media mixed with 2 ml fresh medium. After 16 h, the media were changed and the cells were cultured for a further 48 h. Then, the cells were incubated in culture media containing puromycin (3 μg/ml) for 7 days.

Table 2 ShRNA targeting wild-type of swine IFITM1

Name	Sequence (5′-3′)
IFITM1-shRNA-F	CCGGGGTGTTTGTATACATAACAGCTCAAGAGGCTGT TATGTATACAAACACCTTTTT
IFITM1-shRNA-R	AATTAAAAAGGTGTTTGTATACATAACAGCCTCTTGA GCTGTTATGTATACAAACACC

Construction of IFITM1 C-terminal mutants

IFITM1 wild-type and alanine-scanned gene sequences with Flag-tag fused to the COOH terminus were synthesized for expression in IPEC-J2 cell. Single amino acid alteration was introduced using site-directed mutagenesis kit (TaKaRa, Shiga, Japan). The gene cassette, along with a c-terminal Flag-tag for expressed protein analysis, was cloned into the EcoR I and Xba I sites of the pCI-neo, and desired sequences were confirmed by capillary sequencing. The primers used are shown in Table 3.

Plasmid transfection and virus infection

Cells seeded into 6-well plates were allowed to adhere to the wall overnight, and plasmid transfection was performed when the cell density reached 70%. PEDV infection (MOI = 0.1) was performed 12 h after transfection, and complete medium was replaced 1 h later.

Fluorescence microscopy

IPEC-J2 cells seeded into the 12-well plate with the slides inside were transfected at the cell density of 70%. The transfected plasmid for each well of the 12-well plate was 0.1 μg. 12 h post transfection, PEDV infection (MOI = 0.1) was carried out and incubated in an incubator for 1 h. Immunofluorescence assay (IFA) was performed 24 h after infection. The primary antibodies

Table 3 Primers used for constructing wild-type and mutant porcine IFITM1

Name	Sequence (5′-3′)
IFITM1-WT-F	GGAATTCCATGATCAAGAGCCA
IFITM1-WT-R	GCTCTAGATTACTTATCGTCGTCATCCTTGTAATCGTAGCCTCTGTT
AA107-F	GTGTTTGCAGCAGCAGCAGCACAGATGTTAGAGCGCGCA
AA107-R	CATCTGTGCTGCTGCTGCTGCAAACACCAGAAGAACAGT
AA113-F	GCAGCAGCAGCAGCAGCAAAGAGTAACAGAGGCTACGATTACAAGG
AA113-R	TGCTGCTGCTGCTGCTGCGTAGGCTGTTATGTATACAAACACCAGA
AA119-F	GCAGCAGCAGCAGCAGCAGATTACAAGGATGACGACGATAAGTAA
AA119-R	TGCTGCTGCTGCTGCTGCTGCGCGCTCTAACATCTGG
Q113A-F	AGCCTACGCAATGTTAGAGCGCGCAAAGAGTA
Q113A-R	CTAACATTGCGTAGGCTGTTATGTATACAAACACCAGA
M114A-F	CTACCAGGCATTAGAGCGCGCAAAGAGTAACA
M114A-R	GCTCTAATGCCTGGTAGGCTGTTATGTATACAAACACC
L115A-F	TACCAGATGGCAGAGCGCGCAAAGAGTAACAGA
L115A-R	CGCTCTGCCATCTGGTAGGCTGTTATGTATACAAAC
E116A-F	GATGTTAGCACGCGCAAAGAGTAACAGAGGCT
E116A-R	TTGCGCGTGCTAACATCTGGTAGGCTGTTATGTATACAA
R117A-F	GTTAGAGGCAGCAAAGAGTAACAGAGGCTACGATT
R117A-R	TCTTTGCTGCCTCTAACATCTGGTAGGCTGTTATGTATA

were mouse anti-PEDV (1:200) and rabbit anti-IFITM1 (1:200). The secondary antibody was donkey anti-rabbit 594 fluorescent secondary antibody (1:2000) and Donkey Anti-Rat 488 (1:2000). Subcellular localization of PEDV and IFITM1 was determined by using fluorescence microscopy.

Quantitative real-time PCR assay (RT-qPCR)

Total RNAs were isolated by using TRIzol Reagent (TaKaRa, Shiga, Japan) and subjected to cDNA synthesis with the PrimeScript RT Reagent Kit (TaKaRa). RT-qPCR was performed in triplicate by using SYBR Premix Ex Taq (TaKaRa), and the data were normalized with the level of β-actin expression in each individual sample. Melting curve analysis indicated the formation of a single product in all cases. The $2^{-\Delta\Delta Ct}$ method was used to calculate relative expression changes. For quantification of PEDV genome copy number, a 489 bp PCR product of the PEDV M gene was cloned into pET28a vector. Serial tenfold dilutions of this plasmid were used to construct a standard curve. The total number of PEDV genomic equivalents was determined by comparison with the standard curve. Primers used for RT-qPCR are presented in Table 4.

Table 4 The detection primers of RT-PCR

Name	Sequence (5′-3′)
Q-GADPH-F	AGGGCATCCTGGGCTACACT
Q-GADPH-R	TCCACCACCCTGTTGCTGTA
Q-IFN-α-F	GCTGCCTGGAATGAGAGCC
Q-IFN-α-R	TGACACAGGCTTCCAGGTCCC
Q-IFN-β-F	CATCCTCCAAATCGCTCTC
Q-IFN-β-R	TCATCCTATCTTCGAGGCAA
Q-IFN-γ-F	CTTCAAAGATAACCAGGCCATT
Q-IFN-γ-R	CGAAGTCATTCAGTTTCCCAGA
Q-IFN-λ-F	CCACGTCGAACTTCAGGCTT
Q-IFN-λ-R	CCACGTCGAACTTCAGGCTT
Q-IL-1β-F	GAGCATCAGGCAGATGGTGT
Q-IL-1β-R	AAGGATGATGGGCTCTTCTTC
Q-IL-18-F	TCTACTCTCTCCTGTAAGAAC
Q-IL-18-R	CTTATCATGTCCAGGAAC
Q-IFITM1-F	CTGGGCTTCGTGGCTTTC
Q-IFITM1-R	AACAGTGGCTCCGATGGTC
Q-IFITM2-F	TCGTCTGGTCCCTGTTCAACACCC
Q-IFITM2-R	ACAGTGGCTCCGATGGTCAGAATG
Q-IFITM3-F	GAATTGCGCTTCCCAGCCCTTCTT
Q-IFITM3-R	GGAGGTCTCGCTTCGGATGTTGAT
Q-PEDV-F	GGTGGTCTTTCAATCCT
Q-PEDV-R	AGCCCTCTACAAGCAAT

Immunoblotting analysis

Whole-cell lysates were extracted with lysis buffer (50 mM Tris HCl, pH 8.0, 150 mM NaCl, 1% Triton X-100, 1% sodium deoxycholate, 0.1% SDS, 2 mM $MgCl_2$) supplemented with protease and phosphatase inhibitors (Roche, Mannheim, Germany). The protein concentrations in the lysates were quantified with a BCA Protein Assay Kit (DingGuo, Beijing, China) on a microplate reader (Awareness Technology Inc., Palm City, FL, USA). Protein samples (50 μg) were separated by SDS-PAGE, transferred to nitrocellulose membranes (Millipore, Billerica, MA, USA), and incubated in 5% nonfat milk (Sangon, Shanghai, China) for 1 h at room temperature. The membranes were incubated with primary antibody overnight at 4 °C and then with a horseradish-peroxidase-conjugated, donkey anti-mouse IgG antibody (diluted 1:5000) for 1 h at room temperature. Primary antibodies used were anti-Flag mouse monoclonal antibody (1:1000), anti-Myc mouse monoclonal antibody (1:1000), anti-IFITM rabbit monoclonal antibody (1:10), anti-PEDV S protein mouse monoclonal antibody and anti-β-actin mouse monoclonal antibody (1:10000, Sigma). Immunoblotting results were visualized using Luminata Crescendo Western HRP Substrate (Millipore) on GE AI600 imaging system (Boston, MA, USA).

Immunogold labeling

IPEC-J2 cells were transfected with pCI-IFITM1 plasmid or empty plasmid, 36 h post transfection, supernatant purified by ultracentrifugation through a 25% sucrose cushion were harvested, collected onto carbon coated nickel grids. Grids were incubated with anti-Flag antibody, after extensive washing, grids were then incubated with gold-conjugated goat-anti-mouse IgG (5 nm, Sigma). Following washing, developer was applied to Grids.

Cell activity analysis

Cells were seeded at 10^4 per well in 96-well/plate and viability was determined using MTT assay.

$TCID_{50}$ assay

The virus titer was determined using the $TCID_{50}$ method. IFITM1, IFITM3 and IFITM1/3 were transfected into IPEC-J2 cells, and PEDV was added 24 h later. 48 h later, the virus supernatant was collected and $TCID_{50}$ was measured with vero cells. Vero cells were seeded in 96-well plates at a ratio of 1×10^4 cells/well. 100 μl of serially diluted (10^{-1} to 10^{-10}) viral suspension in 2% DMEM were inoculated in triplicated onto vero monolayer cells,

and incubated for 1 h at 37 ℃. The normal cells served as mock control. Incubate for 24 h at 37 °C and calculate $TCID_{50}$ according to the Reed-Muench formula.

Co−immunoprecipitation (CO−IP)

293 T cells were cultured in 6-well plates. The cells were co-transfected by multiple plasmids (IFITM1, PEDV-N, PEDV-M, PEDV-E, PEDV-ORF3). After 48 h, cells were collected and lysed in 0.2 mL of RIPA buffer. 0.2 mL of anti-Flag, anti-Myc, or control IgG antibody diluted in 200 μL PBS with Tween™ 20 and 50 μL of Dynabeads™ magnetic bead (Invitrogen, USA) for 2 h to 3 h at room temperature. Place the tube on the magnet and remove the supernatant. Add the lysates and gently pipette to resuspend the magnetic bead-Ab complex for 4 h to 6 h at 4 ℃. The Sepharose beads were washed three times with 200μL of Washing Buffer. Remove the supernatant and add 50 μL of 2×SDS sample buffer. Immunoprecipitation was followed by Western blotting with anti-Flag and anti-Myc antibodies.

Statistical analysis

All data were analyzed using the Prism 5 software (GradphPad Software, La Jolla, CA, USA). All data were analyzed with two tailed Student's t-test. $P<0.05$ was considered statistically significant.

Results

PEDV infection promotes the expression of immune-related cytokines in IPEC-J2 cells

IPEC-J2 cells were infected with PEDV strain JS2008 at an MOI of approximately 0.1, while untreated cells were included as a control. Total RNAs were extracted from cells harvested at the indicated time points, and reverse-transcribed into cDNAs as the template for fluorescent quantitative PCR. After comparative analysis with internal reference GAPDH, the viral RNA content was defined as 1 when the cells were infected for 6 h, and the fold alterations of viral RNAs in cells at different times were determined. As indicated in Fig. 1A, the viruses began to rapidly proliferate 6 h post infection, and peaked at 24 h, then gradually decreased in the following time period. Consequently, the mRNA expression levels of multiple cytokines including IFN-α, IFN-γ, IFN-λ, interleukin 1β (IL-1β) and interleukin 18 (IL-18) in PEDV infected IPEC-J2 cells were pronouncedly changed, although the altered pattern was totally different. Briefly, the expression of these examined genes experienced an upregulated and downregulated process, with IFN-α and IFN-β peaking at 6 h, IL-18 peaking at 12 h while IFN-γ, IFN-λ and IL-1β reaching to the highest at 24 h and 48 h, respectively (Fig. 1B–G), suggesting that PEDV infection can induce the expression of cytokines. Besides this, PEDV infection also triggered an early upregulation of pIFITM1, whereas the expression of pIFITM3 was induced to a higher level only at the late time (Fig. 1H and I), indicating that PEDV-induced expression of IFITMs varies, depending on protein types.In addition, the protein levels of IFITMs after PEDV infection were evaluated, and the results were consistent with the mRNA changes(Fig. 2A), indicating PEDV infection promotes the expression of IFITM1 in IPEC-J2 Cells.

pIFITM1 stable cell line inhibit PEDV virus replication

IFITMs is a key cytokine capable of inhibiting a variety of viruses, and we speculated that IFITMs expression could inhibit PEDV replication. Meanwhile, IFITMs family includes IFITM1/2/3, which have different antiviral mechanisms, so we constructed a cell line stably expressing pIFITM1/2/3 (Fig. 2B). It was found that the single expression of pIFITM1 and the co-expression of multiple pIFITM1/2/3 did not affect the expression of pIFITM1. To explore pIFITM1 two-thirds/function of inhibiting viral replication, and we will express pIFITM1 stability, pIFITM1/2, pIFITM1/3, pIFITM1/two-thirds of cell line respectively PEDV infection/after 48 h, 24 h As proved by RT-qPCR, pIFITM1 can significantly reduce PEDV replication at late 48 h, and pIFITM2/3 has an enhanced antiviral effect on pIFITM1 (Fig. 2C and D). This indicates that pIFITM1 has the ability to inhibit PEDV replication, and PIFITM1/2/3 has a synergistic effect. In addition, we collected the cell supernatant after 48 h to detect the $TCID_{50}$ of PEDV (Table 5), which also indicated that pIFITM1 could significantly inhibit PEDV replication (Fig. 2F).

The knockdown of pIFITM1 enhances PEDV infection

To further verify the role of pIFITM1 in suppressing PEDV infection, we generated IFITM1 stably knockdown IPEC-J2 cells by using Lentivirus-mediated shRNA delivery. One independent shRNA specifically targeting pIFITM1 (shIFITM1) showed significant knockdown efficiency, as proven by RT-qPCR (Fig. 3A). MTT assay revealed that the cell viability was not affected by pIFITM1 downregulation (Fig. 3B).Subsequently, WB experiment was used to verify the infection efficiency of shIFITM1 plasmid (Fig. 3C). In contrast to almost no effect 24 h post infection, after viral challenge 48 h, the downregulation of IFITM1 greatly promoted the 1.1-fold of PEDV infection compared to the NC group, as revealed by RT-qPCR analysis (Fig. 3D and E). This further validates the crucial function of IFITM1 in repressing PEDV infection.

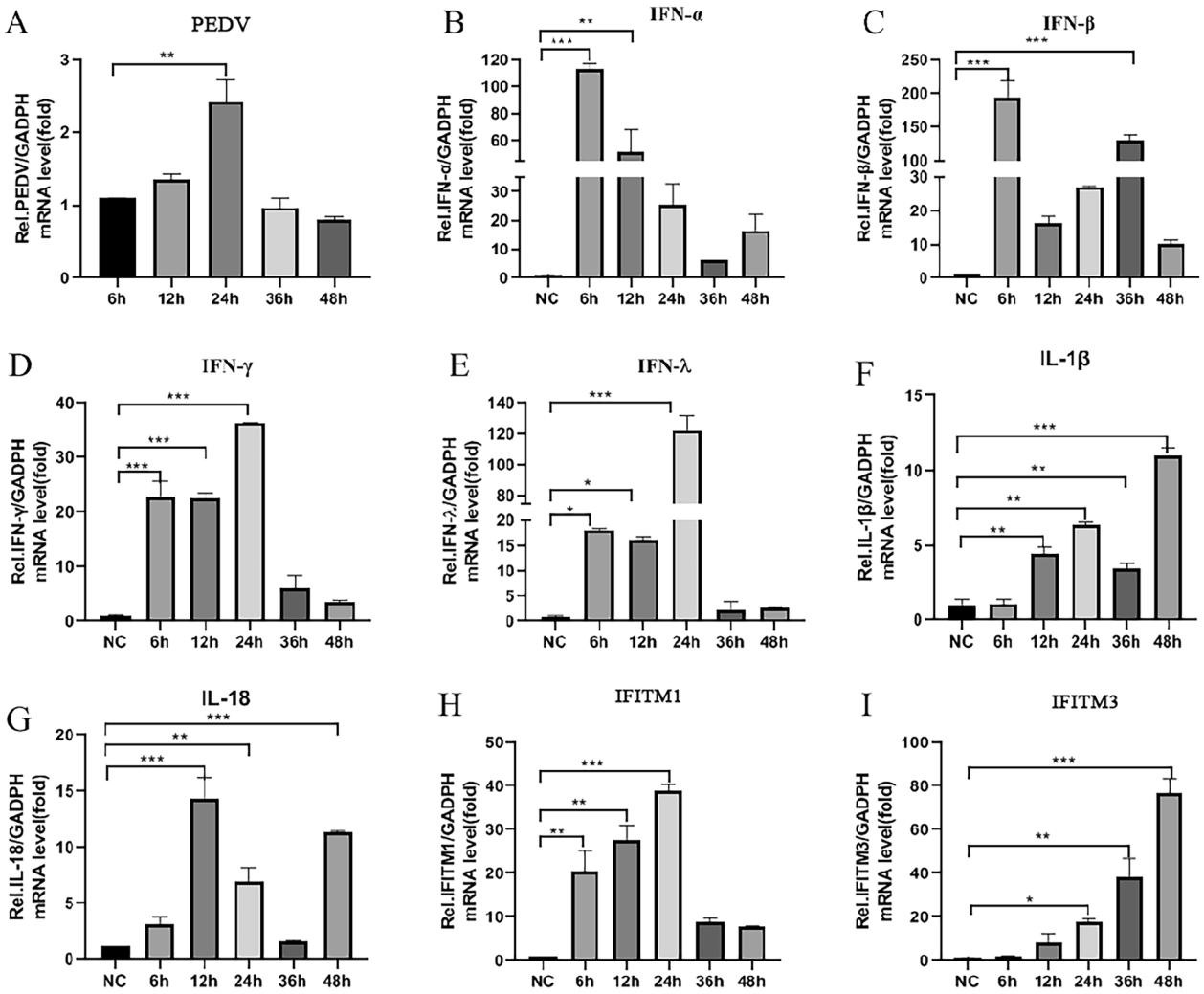

Fig. 1 Changes in the expression of immune-related cytokines after PEDV infection. **A** The mRNA level of PEDV at different time points; **B** IFN-α mRNA level; **C** IFN-β mRNA level; **D** IFN-γ mRNA level; **E** IFN-λ mRNA level; **F** IL-1β mRNA level; **G** IL-18 mRNA level; **H** IFITM1 mRNA level; **I** IFITM3 mRNA level. (*$P < 0.05$; **$P < 0.01$; ***$P < 0.001$.n = 3)

The localization of IFITM1 and PEDV

To address how IFITM1 affects the infection of PEDV, we analyzed their subcellular localization or distribution. Fluorescence microscope observation revealed that following PEDV infection, IFITM1 aggregation was observed at the midpoint of cytoplasm in the control cells in the absence of obviously altered IFITM1 expression, while in the IFITM1 overexpressed cells, it was distributed around the nucleus. Furthermore, colocalization of it with PEDV could be identified, as shown in Fig. 4A. And through IFA and CO-IP experiments, it was found that IFITM1 interacts with the N protein of PEDV, indicating that IFITM1 may bind to N protein to influence PEDV infection (Fig. 4B and C).

Amino acids in the c-terminal domain of IFITM1 are important for its functionality.

The currently established model of the IFITM1 structure manifests its short N-terminal domain resided in the cytoplasm, two membrane domains linked by a conserved intracellular loop (CIL) exposed to the cytoplasm, and the CTD exposed on the cell surface. It is reasonable to speculate that mutations in this CTD domain may alter IFITM1 localization, thereby affecting its functionality. To validate this notion, we created several constructs in which, 6 consecutive amino acids (AAs) starting from the first C-terminal AA of IFITM1 were substituted by corresponding alanines (A) (Fig. 4D). The expression of these mutated proteins

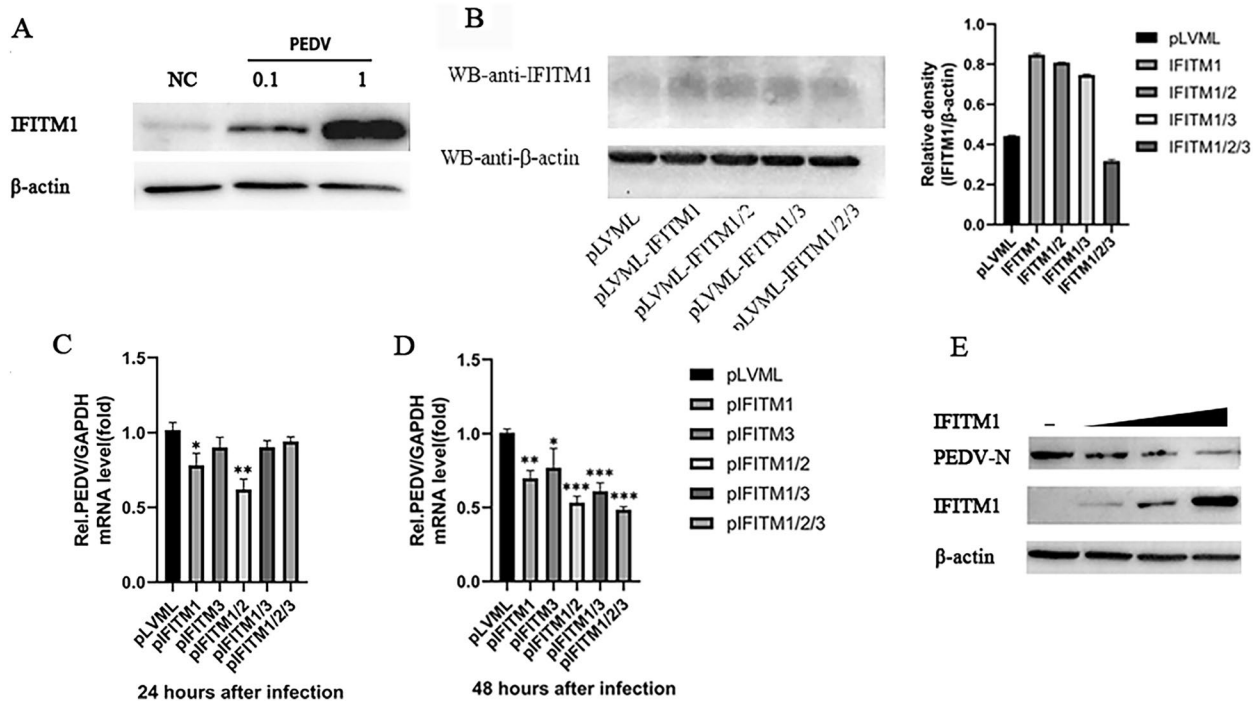

Fig. 2 Stable expression of pIFITM1/2/3 cell lines inhibited PEDV replication. **A** The expression of IFITM1 in PEDV with MOI of 0.1 and 1 by Western blotting; **B** The expression of IFITM in the pIFITM1/2/3 stable cell line by Western blotting; **C**–**D** Effect of stable expression of pIFITM1/2/3 cell lines on PEDV proliferation at 24 h/48 h; **E** N protein expression of PEDV when IFITM1 overexpression was 0/250/500/1000 ng by Western blotting. (*$P<0.05$; **$P<0.01$; ***$P<0.001$. n = 3)

Table 5 Determination of PEDV $TCID_{50}$

	NC	IFITM1	IFITM3	IFITM1/3
$TCID_{50}$/ml	5.85×10^{7}	5.01×10^{7}***	4.38×10^{7}***	4.88×10^{6}***

* $P<0.05$

** $P<0.01$

*** $P<0.001$

n = 3

in IPEC-J2 cells was confirmed by immunoblotting using an antibody against the C-terminal FLAG tag (Fig. 4E). Interestingly, it seemed that the protein size of IFITM1 AS107 mutant was smaller than wild-type IFITM1, while the protein expression levels of IFITM1 AS107 and AS119 mutants were higher than that of wild-type IFITM1. IPEC-J2 cells were then transfected with these constructs or empty vector (as control), and followed by PEDV infection. Enhanced expression of IFITM1 AS-107 and AS-113 mutants reduced attachment of PEDV when compared with wild-type IFITM1 overexpression at the early stage (Fig. 4F and G). However, the occurrence of increased PEDV infection was observed in cell lines expressing the IFITM1 AS-107 and 119 mutants (Fig. 4H and I) suggesting an impairment of IFITM1-mediated restriction of PEDV infection. In order to explore whether the amino acid replacement of IFITM1 will affect the interaction with PEDV N protein, we conducted CO-IP experiments on mutant IFIMT1 and N protein. the results showed that AS107 and AS113 could not interact, while AS119 still had interaction phenomenon (Fig. 4J). These results demonstrate that IFITM1 can restrict PEDV infection, while AA sequence alterations in the CTD severely compromise this function. In addition, we selected TGEV, another existing coronavirus strain, to explore whether IFITM is related to the N protein of other coronaviruses, and found that IFITM 3 can also interact directly with the N protein of TGEV(Fig. 4K), which indicates that IFITM may have a direct effect on the N protein of most coronaviruses, and thus exert its antiviral effect.

In order to further address the contribution of the CTD to the antiviral function of IFITM1, 5 site-directed mutant constructs were generated, with individual AA alteration at the positions of 113–117 in the IFITM1 CTD (Fig. 5A), thereby facilitating to reveal the key site. The expression of these new IFITM1 mutants in IPEC-J2 cells was verified by Western blotting, with varying protein levels (Fig. 5B). Notably, the switch of

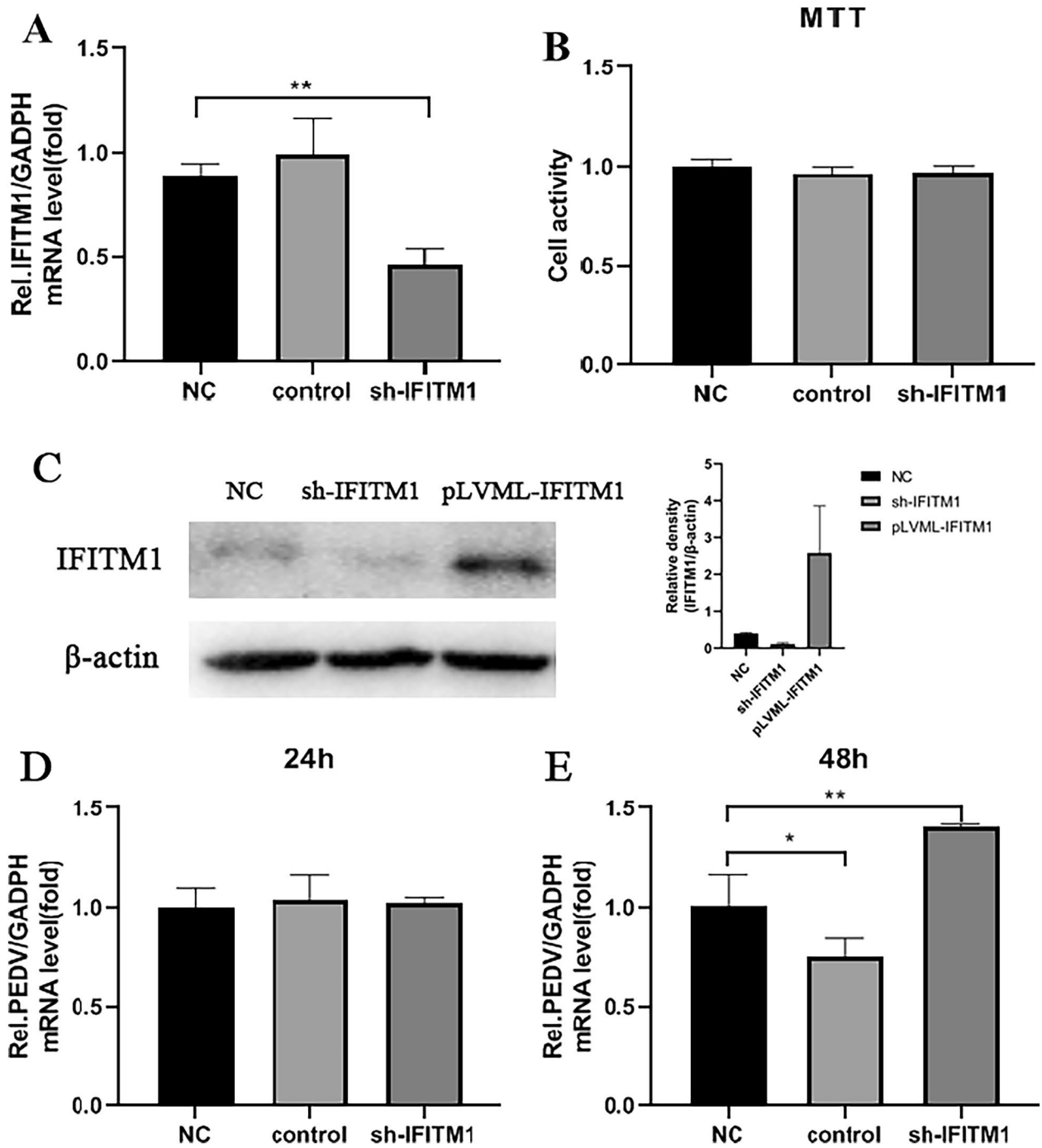

Fig. 3 Interference with IFITM1 expression promotes PEDV infection. **A** IFITM1 mRNA level in knockdown cell line; **B** The viability analysis of IFITM1 knockdown cell line; **C** we harvested the pLVML-IFITM1 and sh-IFITM1 J2 cells at 48 h. Endogenous IFITM1 expression was determined by Western blot.; **D**–**E** The mRNA level of PEDV in knockdown cell line. (*$P < 0.05$; **$P < 0.01$; ***$P < 0.001$. n = 3)

arginine to alanine at 117 led to less protein content of IFITM1. Importantly, IFITM1 mutants with altered AA at 113 and 117 sites enhanced the amount of viruses at the time point of 30 min after PEDV adsorption, while all mutants presented an markedly inhibitory effect on PEDV attachment, as indicated by reduced amount of viruses relative to that of wild-type IFITM1 at the time point of 1 h after PEDV inoculation (Fig. 5C and D). In contrast to no or less effect of the AA at the 113 site, the other AAs at the positions of 114–117 severely affected

the antiviral action of IFITM1, as demonstrated by significantly increased PEDV proliferation in IPEC-J2 cells transfected with these constructs (Fig. 5E and F). These data show that the region including 114–117 AAs are essential for IFITM1 normal functionality.

IFITM1 is embedded into PEDV budding virions

To confirm that nascent PEDV viral particles could recruit IFITM1, cryo-EM was performed on cells expressing IFITM1 using anti-Flag antibodies conjugated to gold beads, negative control consisted of cells transfected with vector DNA. Interestingly, the results indicated that IFITM1 protein is indeed present at sites of PEDV budding (Fig. 6A), and the expression of IFITM1 was also validated by immunoblotting using an antibody against the IFITM1 (Fig. 6B). The experimental results showed that the gold particles represented IFITM1, and the gold particles could attach to the surface of the virus particles under electron microscopy, which proved that IFITM1 was also embedded on the surface of the virus. Meanwhile, the purified virus was verified by Western blotting, and the experimental results also hatched bands. In conclusion, IFITM1 is embedded into PEDV budding virions.

In order to exposit that after IFITM1 is integrated into PEDV virus particles, 293 T cells were transfected with pCI-IFITM1 over-expression plasmid. PEDV infection (MOI = 0.1) was performed 12 h after transfection. the supernatants of the cells collected after 60 h, and IPEC-J2 cells were used for secondary infection. After 48 h, the PEDV M gene transcription was detected by relative qPCR. Accordingly, Compared with the NC group, the transcription level of PEDV M gene in the PCI-IFITM1 group was significantly reduced by more than half (Fig. 6C).

Discussion

Pigs of all ages are susceptible to PEDV infection, moreover, neonatal mortality can be as high as 100%. Due to PEDV high mutation rate, its related vaccines fail to completely prevent and control porcine epidemic diarrhea, rendering the occurrence of this disease still to be frequent and serious [15]. Innate immunity is the most direct and effective way for organisms to prevent and block viral infection [3]. This allows antiviral factors including IFITMs and the underlying mechanisms to be important research hotspots in the field of innate immunity [11].

This study provided robust evidence to demonstrate that PEDV infection could activate innate immunity, as indicated by elevated expression of several IFNs, IL-1β and IL-18 in IPEC-J2 cells. Furthermore, PEDV infection triggered increased level of IFITM1, while the latter's overexpression could suppress the infection of the former. Similar phenomena were also reported in other coronaviruses. For instance, IFITM1 could restricted the entry process of MARV and EBOV [12], SARS-CoV-2 [4]. Deletion of the carboxyl-terminal 12 amino acid residues from IFITM1 enhanced the entry of MERS-CoV and HCoV-OC43 [28].

The antiviral mechanisms of IFITMs remain to be further investigated. Our finding indicated that IFITM1 protein could be embedded on the surface of PEDV viral particles, as revealed by immunocolloidal gold electron microscopy and further confirmed by Western Blot. Similar phenomenon has been observed in HIV reported by a previous study, which indicated the inhibitory action of IFITM3 on the invasion of HIV was also mediated by this way [25]. We found through the CO-IP experiment that IFITM1 can bind to the N protein of PEDV, indicating that IFITM1 may inhibit virus invasion through certain reactions during the release of nucleic acid during virus invasion. Whether this is a common antiviral mechanism of IFITMs requires further investigations.

Additionally, we found that some mutations at the CTD of IFITM1 could alter its anti-PEDV function, as demonstrated by reduced PEDV adsorption at the early stage while increased PEDV proliferation at the late stage in these IFITM1 mutant introduced cells, with the amino acids at position 114–117 (MLER) having an important influence. This finding was in accordance with previous studies, which indicated that some key structural motifs or residues even determine the biological activities of IFITMs. One study showed that removal of the C-terminal 18 amino acid residues of IFITMs efficiently promoted HCoV-OC43 infection [27], similarly, another

(See figure on next page.)

Fig. 4 The IFITM1 CTD is necessary for its antiviral action. **A** The localization of IFITM1 and PEDV after viral infection by fluorescence microscopy; **B** The localization of IFITM1 and PEDV-N by fluorescence microscopy; **C** 293 T cells were transfected with 2 μg PCI-PEDV-N along with the 2 μg PCI-IFITM1. Cell lysates were subjected to IP using IgG, anti-HA, or anti-Flag primary antibody and detected with Western blot using the indicated antibody. The protein samples as input were subjected to Western blot. **D** Strategies for creating IFITM1 mutants with continuous substitution of its C-terminal domain; **E** Identification of the expression of recombinant wild type and CTD mutated IFITM1 by Western blotting; **F**–**G** Effects of transient overexpression of WT and mutant IFITM1 on PEDV infection at the attachment stage at 4 ℃ for 30 and 60 min; **H**–**I** Effects of IFITM1 c-terminal mutants on PEDV proliferation; **J**–**K** CO-IP. (*$P < 0.05$; **$P < 0.01$; ***$P < 0.001$. n = 3)

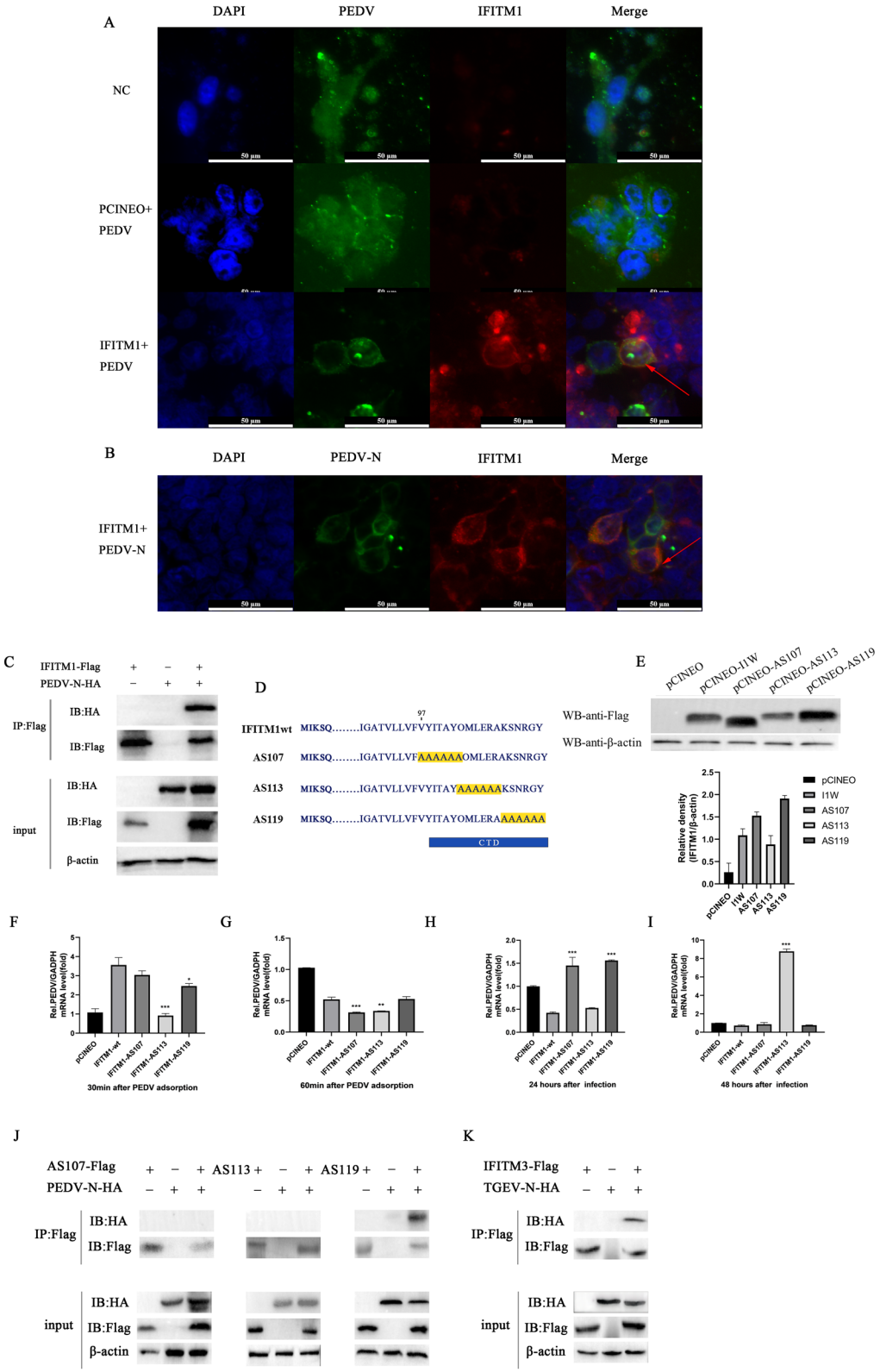

Fig. 4 (See legend on previous page.)

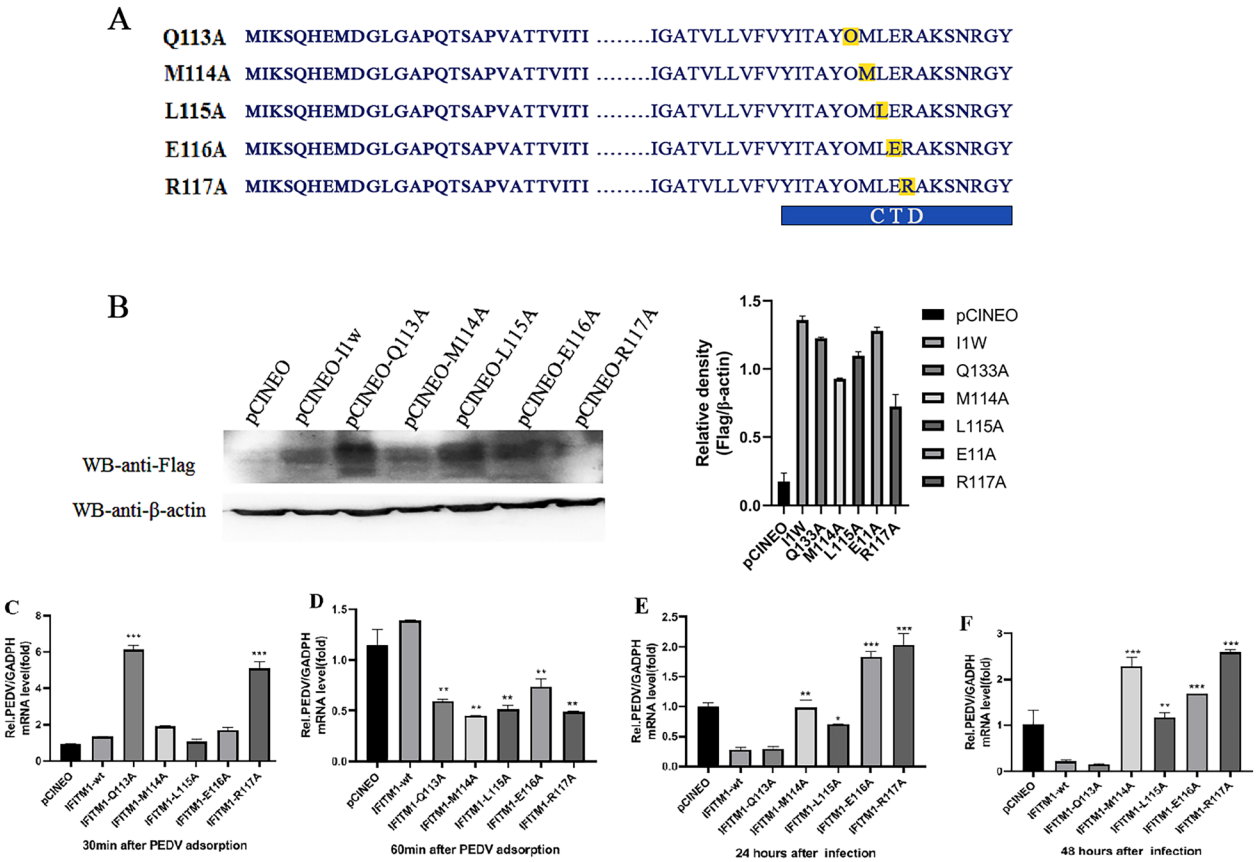

Fig. 5 Antiviral functional amino acid analysis of IFITM1 on PEDV infection. **A** Site-directed mutagenesis strategy at the C-terminal domain of IFITM1; **B**–**C** Identification of the expression of C-terminal site-directed mutated IFITM1 by Western blotting; **D–E** Effects of transient overexpression of IFITM1C-terminal mutants on PEDV infection at the attachment stage; **F–G** Effects of IFITM1 with C-terminal site-specific mutagenesis on PEDV proliferation. (*$P < 0.05$; **$P < 0.01$; ***$P < 0.001$. n = 3)

report demonstrated that deletion of the C-terminal 9 and 12 amino acid residues from IFITM1 enhanced the entry of MERS-CoV and HCoV-OC43 [28]. Though our study and previous reports have identified important functional sites of IFITMs, the specific mechanism of these residues or motifs affecting the antiviral activity of IFITM1 needs to be further investigated.

In summary, this study reveals that (i) PEDV infection induces the expression of immune-related cytokines in IPEC-J2 cells. (ii) IFITM1 is involved in inhibiting the proliferation of PEDV in IPEC-J2 cells, and the C-terminal domain is key determinant for IFITM1 to modulate the replication and proliferation of PEDV. (iii) the embedment of IFITM1 on the surface of virions may reduce the infectivity of nascent PEDV. In conclusion, we for the first time reveal the crucial antiviral role of IFITM1 against PEDV, and provide a new host factor with anti-PEDV action, thereby suggesting IFITMs like IFITM1 can be an effective potential target for the development of novel antiviral drugs.

(See figure on next page.)

Fig. 6 IFITM1 coalesce into PEDV budding virions. **A** IPEC-J2 cells were transfected with IFITM1 and infected by PEDV, analyzed by immuno-gold labeling with anti-Flag antibody. Negative control consisted of cells transfected with vector DNA. Scale bars: 50 nm; **B** cell lysates respectively from IPEC-J2 cells were transfected with PCI-IFITM1 and empty plasmid by immune-gold labeling with anti-Flag antibodies. IPEC-J2 cells were transfected with PCI-IFITM1 and empty plasmid, 36 h later, the supernatants purified by ultracentrifugation through a 25% sucrose cushion were harvested and analyzed by WB with anti-IFITM1 antibodies. **C** 293 T cells were transfected with PCI-IFITM1 and empty plasmid. PEDV infection (MOI = 0.1) was performed 12 h after transfection. the supernatants of the cells collected after 60 h, and IPEC-J2 cells were used for secondary infection. After 48 h, the mRNA level of PEDV determined by relative qPCR. (*$P < 0.05$; **$P < 0.01$; ***$P < 0.001$. n = 3)

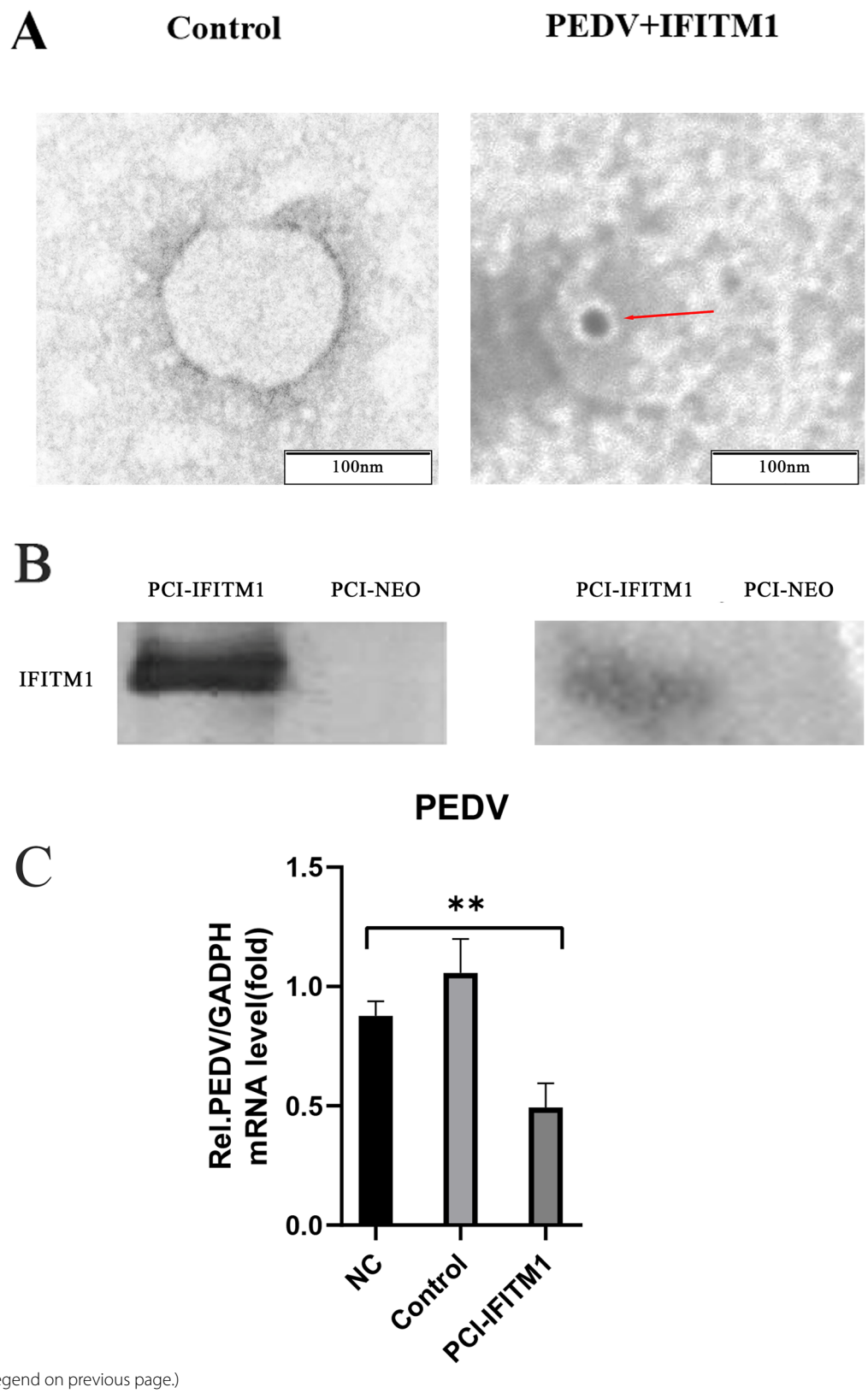

Fig. 6 (See legend on previous page.)

Acknowledgements
We would like to thank our laboratory members who helped us to improve the manuscript with their excellent technical assistance.

Author contributions
Author 1 (first author): conceptualization, methodology, software, investigation, formal analysis, writing—original draft; Author 2: data curation, writing—original draft; Author 3: visualization, investigation; Author 4: resources, supervision; Author 5: investigation; Author 6: visualization Author 7: validation; Author 8: supervision; Author 9: supervision & investigation; Author 10: writing—review & editing; Author 11 (corresponding author): conceptualization, funding acquisition, resources, supervision, writing—review & editing.

Funding
This study was supported by the Outstanding Youth Project of Hunan Provincial Department of Education (22B0224), and the Hunan Provincial Natural Science Foundation of China (2020JJ4041), and the Postgraduate Scientific Research Innovation Project of Hunan Province (CX20200659), and the Natural Science Foundation of Hunan Province(2021JJ30316), and the Youth Fund Project of Hunan Science and Technology Department (2020JJ5248), and the Science and Technology Major Project of Yunnan Province (202202AE090032), and the Changsha Natural Science Foundation (kq2402188), and Science and Technology Innovation 2030- Major Project (2023ZD0404301).

Data availability
No datasets were generated or analysed during the current study.

Declarations

Ethics approval and consent to participate
Not applicable.

Competing interests
The authors declare no competing interests.

Author details
[1]College of Veterinary Medicine, HunanAgricultural University (HUNAU), Changsha, Hunan 410128, China. [2]PCB Biotechnology LLC, Rockville, MD 20852, USA. [3]College of Animal Science, Yangtze University, Jingzhou 434100, China. [4]Institute of Veterinary Medicine, Jiangsu Academy of Agricultural Sciences, Nanjing 210014, Jiangsu, China. [5]Institute of Yunnan Circular Agricultural Industry, Kunming 650201, Yunnan, China. [6]Changsha Green Leaf Bio Technology Co., LTD, Changsha 410119, Hunan, China.

Received: 12 December 2023 Accepted: 27 September 2024
Published online: 05 November 2024

References

1. Amini-Bavil-Olyaee S, Choi YJ, Lee JH, Shi M, Huang IC, Farzan M, Jung JU. The antiviral effector IFITM3 disrupts intracellular cholesterol homeostasis to block viral entry. Cell Host Microbe. 2013;13:452–64.
2. Appourchaux R, Delpeuch M, Zhong L, Burlaud-Gaillard J, Tartour K, Savidis G, Brass A, Etienne L. Functional mapping of regions involved in the negative imprinting of virion particle infectivity and in target cell protection by interferon-induced transmembrane protein 3 against HIV-1. J Virol. 2019. https://doi.org/10.1128/JVI.01716-18.
3. Barrat FJ, Crow MK, Ivashkiv LB. Interferon target-gene expression and epigenomic signatures in health and disease. Nature Immunol. 2019;20:1574–83.
4. Buchrieser J, Dufloo J. Syncytia formation by SARS-CoV-2-infected cells. EMBO J. 2020;39:e106267.
5. Chutiwitoonchai N, Hiyoshi M, Hiyoshi-Yoshidomi Y, Hashimoto M, Tokunaga K, Suzu S. Characteristics of IFITM, the newly identified IFN-inducible anti-HIV-1 family proteins. Microbe Infect. 2013;15:280–90.
6. Compton AA, Bruel T, Porrot F, Mallet A, Sachse M, Euvrard M, Liang C, Casartelli N, Schwartz O. IFITM proteins incorporated into HIV-1 virions impair viral fusion and spread. Cell Host Microbe. 2014;16:736–47.
7. Desai TM, Marin M, Chin CR, Savidis G, Brass AL, Melikyan GB. IFITM3 restricts influenza A virus entry by blocking the formation of fusion pores following virus-endosome hemifusion. PLoS Pathog. 2014;10: e1004048.
8. Diamond MS, Farzan M. The broad-spectrum antiviral functions of IFIT and IFITM proteins. Nat Rev Immunol. 2013;13:46–57.
9. Emerman M, Li K, Markosyan RM, Zheng Y-M, Golfetto O, Bungart B, Li M, Ding S, He Y, Liang C, Lee JC, Gratton E, Cohen FS, Liu S-L. IFITM proteins restrict viral membrane hemifusion. PLoS Pathog. 2013;9: e1003124.
10 Garst EH, Lee H. Site-specific lipidation enhances IFITM3 membrane interactions and antiviral activity. ACS Chem Biol. 2021;16(5):844–56.
11. Gerlach T, Hensen L, Matrosovich T, Bergmann J, Winkler M, Peteranderl C, Klenk HD, Weber F. pH optimum of hemagglutinin-mediated membrane fusion determines sensitivity of influenza A viruses to the interferon-induced antiviral state and IFITMs. J Virol. 2017. https://doi.org/10.1128/JVI.00246-17.
12. Huang IC, Bailey CC, Weyer JL, Radoshitzky SR, Becker MM, Chiang JJ, Brass AL, Ahmed AA, Chi X, Dong L, Longobardi LE, Boltz D, Kuhn JH, Elledge SJ, Bavari S, Denison MR, Choe H, Farzan M. Distinct patterns of IFITM-mediated restriction of filoviruses, SARS coronavirus, and influenza A virus. PLoS Pathog. 2011;7: e1001258.
13. Jia R, Pan Q, Ding S, Rong L, Liu SL, Geng Y, Qiao W, Liang C. The N-terminal region of IFITM3 modulates its antiviral activity by regulating IFITM3 cellular localization. J Virol. 2012;86:13697–707.
14. John SP, Chin CR, Perreira JM, Feeley EM, Aker AM, Savidis G, Smith SE, Elia AE, Everitt AR, Vora M, Pertel T, Elledge SJ, Kellam P, Brass AL. The CD225 domain of IFITM3 is required for both IFITM protein association and inhibition of influenza A virus and dengue virus replication. J Virol. 2013;87:7837–52.
15. Jung K, Saif LJ, Wang Q. Porcine epidemic diarrhea virus (PEDV): an update on etiology, transmission, pathogenesis, and prevention and control. Virus Res. 2020;286: 198045.
16. Lewin AR, Reid LE, Mcmahon M, Stark GR, Kerr IM. Molecular analysis of a human interferon-inducible gene family. Eur J Biochem. 1991;199:417–23.
17. Lin C-M, Saif LJ, Marthaler D, Wang Q. Evolution, antigenicity and pathogenicity of global porcine epidemic diarrhea virus strains. Virus Res. 2016;226:20–39.
18. Lin CM, Annamalai T, Liu X, Gao X, Lu Z, El-Tholoth M, Hu H, Saif LJ, Wang Q. Experimental infection of a US spike-insertion deletion porcine epidemic diarrhea virus in conventional nursing piglets and cross-protection to the original US PEDV infection. Vet Res. 2015. https://doi.org/10.1186/s13567-015-0278-9.
19. Li K, Markosyan RM, Zheng YM, Golfetto O, Bungart B, Li M, Ding S, He Y, Liang C, Lee JC, Gratton E, Cohen FS, Liu SL. IFITM proteins restrict viral membrane hemifusion. PLoS Pathog. 2013;9: e1003124.
20. Shi G, Kenney AD, Kudryashova E, Zani A, Zhang L, Lai KK, Hall-Stoodley L, Robinson RT, Kudryashov DS. Opposing activities of IFITM proteins in SARS-CoV-2 infection. EMBO J. 2021;40: e106501.
21 Smith SE, Busse DC. Interferon-induced transmembrane protein 1 restricts replication of viruses that enter cells via the plasma membrane. J Virol. 2019. https://doi.org/10.1128/JVI.02003-18.
22. Smith S, Weston S, Kellam P, Marsh M. IFITM proteins-cellular inhibitors of viral entry. Curr Opin Virol. 2014;4:71–7.
23. Sun D, Wang X, Wei S, Chen J, Feng L. Epidemiology and vaccine of porcine epidemic diarrhea virus in China: a mini-review. J Vet Med Sci. 2016;78:355–63.
24 Sun F, Xia Z, Han Y, Gao M, Wang L, Wu Y, Sabatier JM. Topology, antiviral functional residues and mechanism of IFITM1. Viruses. 2020. https://doi.org/10.3390/v12030295.
25. Tartour K, Appourchaux R, Gaillard J, Nguyen XN, Durand S, Turpin J, Beaumont E, Roch E, Berger G, Mahieux R, Brand D, Roingeard P, Cimarelli A. IFITM proteins are incorporated onto HIV-1 virion particles and negatively imprint their infectivity. Retrovirology. 2014;11:103.
26. Wang J, Wang CF, Ming SL, Li GL, Zeng L, Wang MD, Su BQ, Wang Q, Yang GY, Chu BB. Porcine IFITM1 is a host restriction factor that inhibits pseudorabies virus infection. Int J Biol Macromol. 2020;151:1181–93.

27. Zhao X, Guo F, Liu F, Cuconati A, Chang J, Block TM, Guo JT. Interferon induction of IFITM proteins promotes infection by human coronavirus OC43. Proc Natl Acad Sci U S A. 2014;111:6756–61.
28. Zhao X, Sehgal M, Hou Z, Cheng J, Shu S, Wu S, Guo F, Le Marchand SJ, Lin H, Chang J, Guo JT. Identification of residues controlling restriction versus enhancing activities of IFITM proteins on entry of human coronaviruses. J Virol. 2018. https://doi.org/10.1128/JVI.01535-17.

Publisher's Note